Light Metals 2012 *Edited by: Carlos E. Suarez*
TMS (The Minerals, Metals & Materials Society), 2012

Evolution of Iron based intermetallic Phases in Al-7wt%Si hypoeutectic alloy

Anton Gorny and Sumanth Shankar
Light Metal Casting Research Centre (LMCRC), Department of Mechanical Engineering, McMaster University
1280 Main Street West, Hamilton, ON, Canada L8S 4L7

Keywords: Al-Si-Fe alloys, High purity, Al-Si-Fe intermetallics, phase diagram

Abstract

This study has methodically characterized the iron based intermetallic phases evolving during solidification of Al-Si binary alloys as a function of solidification cooling rate and and composition of Fe in the alloys. Contrary to the predictions of the evolution of only the β (Al,Si,Fe) in these alloys by all commercial thermodynamic phase diagram simulation tools, the dominant phases were mostly the α (Al,Si,Fe) intermetallic phases and significantly vary in nature and type with the process parameters. The results from this study will further enable better design of the Al-Si alloys with an in-depth understanding of the evolution of the intermetallic phases and methodologies to prevent or modify the same in the final cast components.

Introduction

Al-Si alloys have significant applications in automotive, aerospace, defense and domestic sectors [1]. One of the detrimental impurities in these alloys is Fe which forms several forms of intermetallic phases such as binary phases with Al and ternary phases with Al and Si [2]. Thermodynamic phase diagram simulations reveal that very low concentrations of Fe in the order of 10 to 50 ppm is sufficient to alter the binary Al-Si system to a ternary Al-Si-Fe system [3]. The presence of certain Fe based intermetallic phases in solidified microstructure of cast components of Al-Si commercial alloys prove to be significantly detrimental to the mechanical properties and performance of the component [4, 5]. In this study, the Al-Si-Fe phases evolved during solidification of Al-7wt%Si alloy with 0.25 and 0.5 wt% Fe in them, respectively has been characterized with Scanning Electron Microscopy (SEM) coupled with Energy Dispersive X-Ray (EDX) analysis. The aim of the work is to verify the validity of predictions of these intermetallic phases evolving during solidification by commercial thermodynamic phase diagram software packages. Two cooling rates, namely, 1 and 5 $°C.s^{-1}$ were used for solidification of the alloys.

Background

Most research [6, 7, 8, 9, 10. 11] on understanding the nature and structure of the Fe base intermetallic compounds in Al-Si hypoeutectic casting alloys (Al – 5 to 12.5 wt%Si) [1] have been carried out in complex multi-component commercial alloys. The prolific nature of Fe to form several complex intermetallic phases with most elements in the Al-Si commercial casting alloys throws more confusion than clarity on the nature of these phases observed in the commercial casting alloys. Rivlin et al [12] and Stefaniay et al [13,have presented an in-depth review of the intermetallic phases in the Al rich corner of the Al-Si-Fe ternary alloy phase diagram. However, there is no discussion presented on the evolution of the intermetallic phases during non-equilibrium solidification of Al rich Al-Si-Fe alloys which would have been more pertinent to the understanding the evolution of these intermetallic phases during solidification of commercial Al-Si casting alloys. Gupta [14] carried out diffusion couple experiments between pure solid Fe and liquid Al-12.5wt%Si eutectic alloy to observe and characterize the various Al-Fe-Si intermetallic compounds formed. The intermetallic phases obtain by Gupta [14] would all be terminal and near equilibrium phases and the list of intermetallic phases formed in such a diffusion couple reaction could not be assumed as comprehensive because of several Al-Si-Fe intermetallic phases that could evolve during non-equilibrium solidification conditions experienced during casting these alloys.

Predictions from thermodynamic simulations of solidification of Al-Si-Fe alloys using Scheil-Gulliver solidification criterion show only β-$Al_{4.5}FeSi$ phase as the Fe based intermetallic phase evolving as terminal phase for alloys with 0.05 to 2.3 wt% Fe in them [15, 3, 16, 17, 18, 19]. Figure 1 shows an isopleth of the Al-Si-Fe ternary phase diagram as simulated with the Pandat thermodynamic software with the PanAl8 materials database [19], wherein the phase evolution with the addition of Fe to Al-7wt%Si alloy is shown. Figure 1 show that addition of trace levels of Fe to Al-7wt%Si is sufficient to enable the evolution of the β-$Al_{4.5}FeSi$ intermetallic phase during equilibrium solidification conditions. The two commercially important alloys of Al-7wt%Si with 0.25 wt% and 0.50 wt% Fe, respectively were chosen for this study and shown in Figure 1.

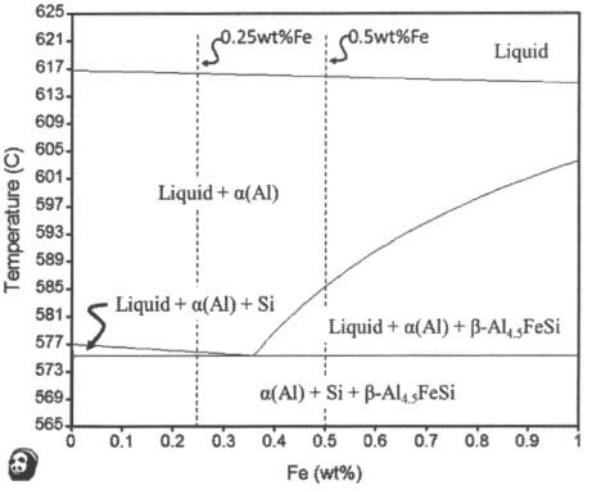

Figure 1: Isopleth of Al-Si-Fe ternary phase diagram showing the effect of Fe addition to Al-7wt%Si alloy. Also shown are the two experiment alloys selected for this study.

Experiments

Alloys were prepared and cast using 99.999% purity Al ingots, 99.9999% purity Si and Al-25%Fe master alloy. Figure 2 shows the schematic of the experimental matrix adopted for this study.

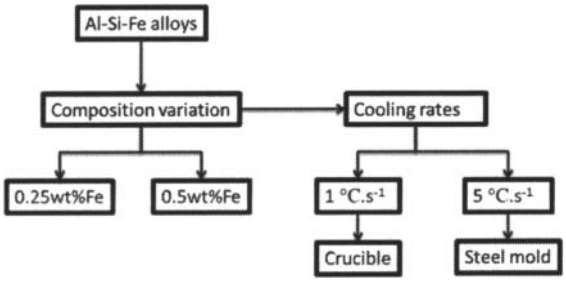

Figure 2: Schematic of the experimental matrix

A ceramic crucible with a coating of Boron Nitride was used to solidify the alloys at 1 and a steel casting mold was used for solidifying alloys at 5 °C.s^{-1}. Al was melt and held for 30 min at 820 °C followed by Si addition and holding time of 30 min; subsequently Fe was added and the alloy was held for an additional 60 min before it was cast into the ceramic crucible or steel mold. On-line temperature data during solidification was collected using two K-type thermocouples such that one was placed at the center (T_C) of the solidifying melt and the other at the outer edge (T_E) of the melt in the same horizontal plane as the first thermocouple [20]; coupled with a laboratory data acquisition system. Specimens from the cast samples were sectioned around the thermocouple regions in the cast samples and prepared for metallographic analysis with a JEOL 7000 Scanning Electron Microscope (SEM) equipped with an Oxford instruments Energy Dispersive X-Ray Spectrometer (EDX).

Results and Discussion

Figure 3 is the typical back scatter electron image (BEI) obtained from the SEM for the Al-7wt%Si-0.25wt%Fe alloy solidified in the ceramic crucible at 1 °C.s^{-1}, showing the dark grey eutectic Si phase and the bright Fe rich intermetallic phases embedded in the Al matrix. In Figure 3, the only Fe based intermetallic phase observed was the α-$Al_{70}Si_{10}Fe_{20}$ whose stoichiometry was determined by EDX in the SEM and this phase is contrary to the one predicted by the Al-Si-Fe phase diagram show in Figure 1. The morphology of the α-$Al_{70}Si_{10}Fe_{20}$ shown in Figure 3 was that of a Chinese script.

Figure 4 shows the typical BEI from the SEM for the Al-7wt%Si-0.25wt%Fe alloy solidified in the steel mold at 5 °C.s^{-1}; wherein the dark grey Si phase and the bright α-$Al_{70}Si_{10}Fe_{20}$ is embedded in the Al matrix. In Figure 4, similar to the slower solidification condition of 1 °C.s^{-1}, only the α-$Al_{70}Si_{10}Fe_{20}$ evolved in the faster solidification condition as well which is contrary to the predictions from the ternary phase diagram shown in Figure 1.

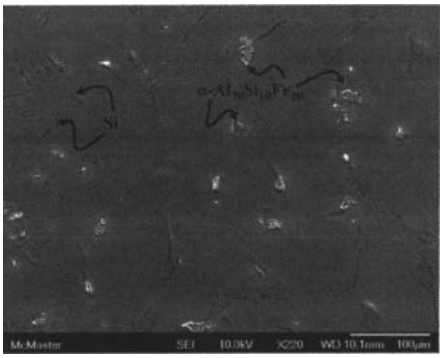

Figure 3: Typical SEM back scatter electron image of Al-7wt%Si-0.25wt%Fe alloy solidified at 1 °C.s^{-1} (ceramic crucible).

The BEIs from the SEM for the Al-7wt%Si-0.50wt%Fe alloy for the two solidification conditions of 1 and 5 °C.s^{-1} are shown in Figure 5 and Figure 6, respectively. In Figure 5, for the slower solidification rate, the β-$Al_{61}Si_{19.5}Fe_{19.5}$ intermetallic phase was solely observed in the solidified microstructure as predicted by the alloy phase diagram in Figure 1. In Figure 6, for the faster solidifying rate, the α-$Al_{70}Si_{10}Fe_{20}$ intermetallic phase was solely observed in the solidified microstructure, contrary to the phase diagram predictions in Figure 1.

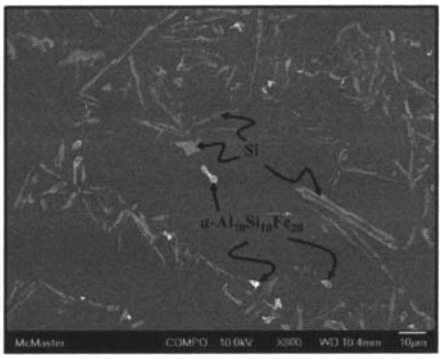

Figure 4: Typical SEM back scatter electron image of Al-7wt%Si-0.25wt%Fe alloy solidified at 5 °C.s^{-1} (steel mold).

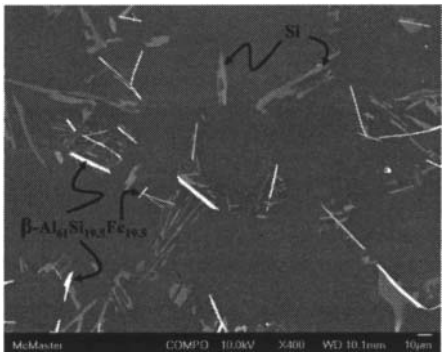

Figure 5: Typical SEM back scatter electron image of Al-7wt%Si-0.50wt%Fe alloy solidified at 1 °C.s^{-1} (ceramic crucible).

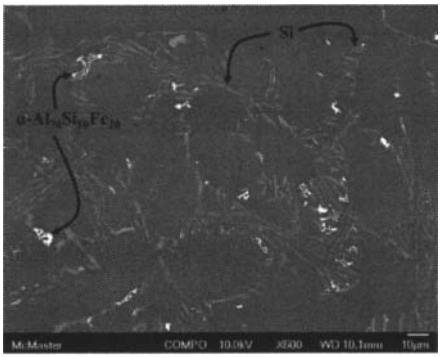

Figure 6: Typical SEM back scatter electron image of Al-7wt%Si-0.50wt%Fe alloy solidified at 5 °C.s^{-1} (steel mold).

Figure 7 (a) and (b) show the typical BEI from SEM of the morphology of the α-$Al_{70}Si_{10}Fe_{20}$ (Chinese script) and β-$Al_{61}Si_{19.5}Fe_{19.5}$ (plates) phases, respectively, as observed in this study.

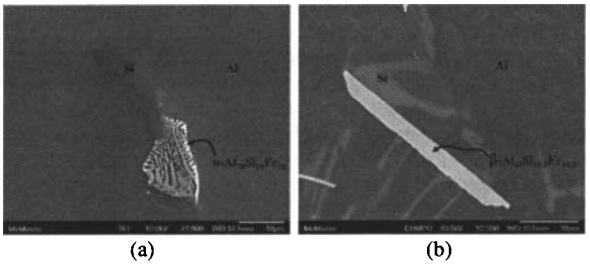

(a) (b)

Figure 7: Typical BEI from SEM of morphology of the two Fe based intermetallic phases observed in this study; (a) α-$Al_{70}Si_{10}Fe_{20}$ and (b) β-$Al_{61}Si_{19.5}Fe_{19.5}$.

Table 1 shows the average composition and standard deviation of the atomic percentage of the respective elements in the Al-Si-Fe intermetallic phase observed in the two alloys at the two solidification conditions, respectively.

Table 1: Average composition of the iron based intermetallic phases obtained by EDS in an SEM for the two alloys in two solidification conditions, respectively.

Fe (wt%) in Al-7wt%Si alloy		0.25	0.25	0.5	0.5
Solidification (°C.s^{-1})		1	5	1	5
Al (at%)	average	**65.94**	**70.75**	**60.9**	**69.25**
	Std. Dev.	0.15	2.65	3.59	2.68
Si (at.%)	average	**11.56**	**10.21**	**19.5**	**10.06**
	Std. Dev.	0.15	1.02	3.38	0.61
Fe (at.%)	average	**22.5**	**20.01**	**19.59**	**20.69**
	Std. Dev.	0.17	1.63	0.24	2.18
number of samples		30	30	30	30
Phase identification [16]		**α**	**α**	**β**	**α**

According to the simulated phase diagram shown in Figure 1, the stoichiometry of the β (Al,Fe,Si) phase is $Al_{4.5}FeSi$, the critical parameter is the ratio of Fe:Si in the stoichiometry which is about 1:1. In this study the stoichiometry of the β (Al,Fe,Si) phase is $Al_{61}Si_{19.5}Fe_{19.5}$ because of the interference of possible inconsistencies in the EDS measurements in SEM due to the interaction volume of the X-Ray beam in the microstructure and the bulk Al matrix with the X-Ray beam. However, it must be noted that the identification of the β (Al,Fe,Si) phase in this study was confirmed by the nearly 1:1 ratio between Fe and Si atoms shown in the results presented in Table 1. A similar argument could be extended to the identification of the α-$Al_{70}Si_{10}Fe_{20}$ phase by the 2:1 ratio between the Fe and Si atoms in the results shown in Table 1. Subsequently, in this manuscript, the two Fe based intermetallic phases shall be referred to as merely α and β.

The phase diagram in Figure 1 shows that for the alloy with 0.25 wt% Fe, the Si phase should evolve prior to the β phase, however, extensive research on the nucleation of the eutectic Si phase in this alloy [3] has shown that the Si phase would not be able to nucleate on the primary Al phase and the temperature of the alloy continues to drop until the β phase evolves by nucleating on the Al phase and followed by the nucleation of the eutectic Si phase on the β phase, under equilibrium solidification conditions of ultra-high purity Al-Si-Fe alloy system as used in this study, as well. In the alloy with 0.50 wt% Fe, the β phase evolves prior to the eutectic Si phase as shown by Figure 1 by nucleating on the primary Al phase, and the Si phase could nucleate on the β phase to complete the solidification.

Figure 3 and Figure 4 show that for the two solidification rates of 1 and 5 °C.s^{-1}, for the Al-7wt%Si-0.25wt%Fe alloy, the predominant intermetallic phase is α and there were some evidences of an unidentifiable Fe based intermetallic phase existing as sub-micron scale bright dots attached to most Si phase in the microstructure as could be observed in these figures. It is our hypothesis that the non-equilibrium solidification conditions of this alloy does not allow for sufficient segregation of the Fe atoms ahead of the solidifying primary α(Al) dendritic front to enable the formation of large phases of the predicted β phase. When the alloy temperature reaches around 577 °C, which is the predicted temperature for the formation of the Si phase by Figure 1, there would be no nucleation event and the alloy undercools to about 575 °C to effect the nucleation of the β phase which would instantaneously lead to the nucleation of the Si phase on itself preventing any further growth of the β phase. Towards the end of the eutectic reaction, the Fe would be segregated in the inter-dendritic liquid and this would result in the formation of an Fe based intermetallic phase with high Fe to Si ratio such as the one observed as 2:1 in the α phase. The ratio is high because most of the Si is consumed by the solidified eutectic Si phase. The α intermetallic phase nucleates on the Si phase as shown by Figure 7 (a). Figure 8 shows the typical thermal curve with the data from the two thermocouples (T_C-T_E) collected during solidification of Al-7wt%Si-0.24wt%Fe alloy in the ceramic crucible at 1 °C.s^{-1}; wherein the evolution of the primary Al phase could be observed at 616 °C and that of the first eutectic phase at 575 °C which according to the Figure 1 and the discussion presented in this paragraph would be the small sub-micron size β phase instantly followed by the Si phase.

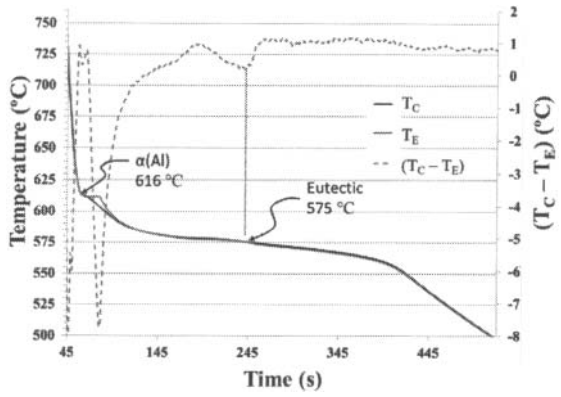

Figure 8: Typical thermal data during solidification of the Al-7wt%Si-0.24wt%Fe in a ceramic crucible (1 °C.s^{-1}).

Figure 5 shows that the predominant intermetallic phase in the microstructure of the Al-7wt%Si-0.50wt%Fe alloy solidified at the slower rate of 1 °C.s^{-1} is the β intermetallic phase (plates). In this solidifying rate, as predicted by the phase diagram in Figure 1, the β phase would evolve at around 586 °C followed by the eutectic Si at around 575 °C. The Figure 5 shows that the Fe based intermetallic phase in this alloy and given solidifying rate is the β intermetallic phase (plates) and it is hypothesized that the solidification rate is slow enough for sufficient segregation of the Fe atoms ahead of the growing primary Al dendrites to effect the nucleation and growth of the β which is subsequently followed by the nucleation and growth of the Si phase at the final eutectic temperature. Figure 9 shows the typical thermal data obtained from the two thermocouples, T_C and T_E during solidification of the Al-7wt%Si-0.50wt%Fe alloy in the ceramic crucible (at 1 °C.s^{-1}); wherein the evolution of the β intermetallic phase at around 590 °C and eutectic Si at around 575 °C are observed and validates the predictions in Figure 1. Figure 7 (b) shows that multiple eutectic Si phase could nucleate on a single plate of β phase whereas the α phase nucleates on a single eutectic Si phase as shown in Figure 7 (a).

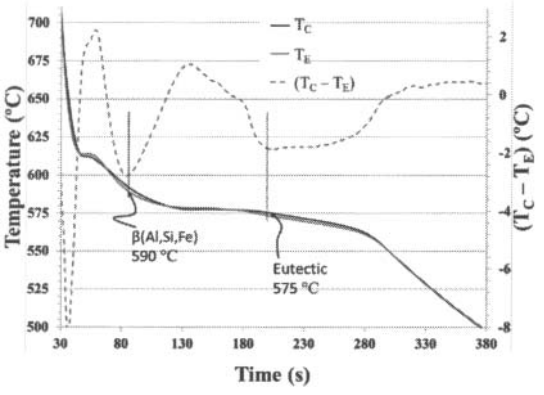

Figure 9: Typical thermal data during solidification of the Al-7wt%Si-0.50wt%Fe in a ceramic crucible (1 °C.s^{-1}).

Figure 6 shows the predominant Fe based intermetallic phase evolving during the solidification of the Al-7wt%Si-0.50wt%Fe alloy in the steel mold at a rate of 5 °C.s^{-1} is the α intermetallic phase. It is our hypothesis that the high solidification rate in the steel mold does not provide sufficient segregation of the Fe atoms ahead of the growing primary Al dendrites to effect the nucleation and growth of the β phase. Hence, as discussed previously, the alloy melt would undercool sufficiently past the predicted nucleation temperature of the β phase (~586 °C) and this phase would evolve close to the eutectic temperature which would instantly trigger the nucleation of the Si phase on the same and thus curtailing the growth of the β phase. The lack of growth of the β phase wold render the final solidifying liquid rich in Fe and depleted in Si and result in the nucleation of the α intermetallic phase with a high ratio of Fe to Si atoms of 1:2 on the eutectic Si phase. This would result in the microstructure observed in Figure 6.

Conclusions

The solidification of the Al-Si-Fe alloy system in the Al rich corner of the phase diagram is quite complex under non-equilibrium conditions such as those observed in casting processes. The Al-7wt%Si alloy with 0.25wt%Fe and 0.50 wt%Fe are commercially important alloys wherein, contrary to the prediction by the thermodynamic simulations of alloy phase diagrams, the terminal phase is not always the β Fe based intermetallic phase. Depending, on the Fe level and the solidification rate, the α Fe based intermetallic phase could also be the terminal intermetallic phase in the solidified microstructure of these alloys. For low levels of Fe in the alloy, the α phase is the terminal phase for a wide range of solidification rates which are akin to those observed to commercial casting processes. Whereas, in higher Fe levels of 0.50 wt% and slower solidification rates which are akin to sand casting processes, the β is the terminal Fe based intermetallic phases present in the solidified microstructure. In the alloys with higher Fe levels of 0.50 wt% and higher solidification rates akin to those observed in the steel mold casting processes, the α intermetallic phase is the terminal phase. The morphology of the α phase is Chinese script and less detrimental to the mechanical properties when compared to the plate morphology of the β phase. This study presents a starting point in our understanding of the Fe based intermetallic phases evolving in this commercially important ternary system and would enable further understanding of the manifestations of the Fe based intermetallic phases due to additional critical alloying elements such as Mg, Mn, Cu and Zn in these alloys.

Acknowledgement

The authors wish to acknowledge the financial support provided by the Ontario Research Fund through the Initiative for Automotive Manufacturing Innovation (IAMI) at McMaster University.

References

1 Joseph R. Davis, J. R. Davis & Associates. 1993. *Aluminum and Aluminum Alloys*. ASM International.

2 S. Takeda, K. Mutuzaki, "The equilibrium diagram of the Fe – Al –Si system", *Tetsu to Hagane*, 26 (1940), 335–361.

3 S. Shankar, Y. W. Riddle and M. M. Makhlouf, "Nucleation mechanism of the eutectic phases in aluminum–silicon hypoeutectic alloys", *Acta Materialia*, 52 (15) (2004), 4447-4460.

4 M. H. Mulazimoglu, A. Zaluska, J. E. Gruzleski, and F. Paray, "Electron microscope study of Al-Fe-Si intermetallics in 6201 aluminum alloy," *Metallurgical and Materials Transactions A*, 27 (4) (Apr 1996), 929-936.
5 G. Gustafsson, T. Thorvaldsson, and G. L. Dunlop, "Microstructure of Cast Al-Si-Mg Alloys," *Metallurgical Transactions*, 17 (Jan 1986), 45-52.
6 M. Warmuzek and A. Gazda, "An analysis of cooling rate influence on the sequence of intermetallic phases precipitation in some commercial aluminium alloys," *J. Anal. At. Spectrom.*, 14 (3) (1999), 535–537.
7 M. Warmuzek, J. Sieniawski, K. Wicher, and G. Mrowka, "The study of the distribution of the transition metals and Si during primary precipitation of the intermetallic phases in Al–Mn–Si alloys," *Journal of Materials Processing Technology*, 175 (1-3) (Jan 2006), 421-426.
8 S. Pontevichi, F. Bosselet, F. Barbeau, M. Peronnet, and J. C. Viala, "Solid-Liquid Phase Equilibria in the Al-Fe-Si System at 727 °C," *Journal of Phase Equilibria & Diffusion*, 25 (6) (Dec 2004), 528-537.
9 C. Dinnis, J. Taylor, and a Dahle, "As-cast morphology of iron-intermetallics in Al–Si foundry alloys," *Scripta Materialia*, 53 (8) (Oct 2005), 955-958.
10 M. Kral, "Identification of intermetallic phases in a eutectic Al/Si casting alloy using electron backscatter diffraction pattern analysis," *Scripta Materialia*, 51 (3) (Aug 2004), 215-219.
11 M. V. Kral, P. N. H. Nakashima, and D. R. G. Mitchell, "Electron microscope studies of Al-Fe-Si intermetallics in an Al-11 Pct Si alloy," *Metallurgical and Materials Transactions A*, 37 (6)(Jun 2006), 1987-1997.
12 V. Rivlin, "4: Critical evaluation of constitution of aluminium-iron-silicon system," *International Metals Reviews*, 3 (1981), 133-152.
13 V. Stefaniay and A. Griger, "Intermetallic phases in the aluminium-side corner of the AlFeSi-alloy system," *Journal of Materials science*, 22 (2) (Feb 1987), 539-546.
14 S. Gupta, "Intermetallic compound formation in Fe–Al–Si ternary system: Part I," *Materials Characterization*, 49 (4) (Nov 2002), 269-291.
15 M. Makhlouf, "The aluminum–silicon eutectic reaction: mechanisms and crystallography," *Journal of Light Metals*, 1 (4) (Nov 2001), 199-218.
16 W. Khalifa and F. Samuel, "Iron intermetallic phases in the Al corner of the Al-Si-Fe system," *Metallurgical and Materials*, 34 (3) (Mar 2003), 807-825.
17 L. Lu and a K. Dahle, "Iron-rich intermetallic phases and their role in casting defect formation in hypoeutectic Al-Si alloys," *Metallurgical and Materials Transactions A*, 36 (3) (Mar 2005), 819-835.
18 Thermocalc, A thermodynamic simulation software, TTAl6 materials database,
19 Pandat, A thermodynamic simulation software, PanAl8 database, Computherm LLC., Madison, WI, USA.
20 L. Bäckerud, E. Król and J. Tamminen, Solidification Characteristics of Aluminum Alloys, volume 1, Universitetsforlaget, Oslo (1986).